

# NMR Spectroscopic Studies of Intrinsically Disordered Proteins at Near-Physiological Conditions\*\*

Sergio Gil, Tomáš Hošek, Zsófia Solyom, Rainer Kümmerle, Bernhard Brutscher, Roberta Pierattelli, and Isabella C. Felli\*

Intrinsically disordered proteins (IDPs) have recently attracted the attention of the scientific community because of their peculiar features that expand our view of how protein function is determined by the conformational properties of a polypeptide chain. The discovery of numerous physiological functions performed by IDPs has challenged the traditional structure–function paradigm.<sup>[1–4]</sup> The lack of a unique stable 3D structure and the high extent of local mobility provide functional advantages to IDPs in terms of structural plasticity and binding promiscuity.

Among the experimental techniques available to obtain atomic-resolution information on IDPs, solution-state NMR spectroscopy plays a predominant role. As a spectroscopic method, NMR is equally well applicable to structured as well as highly disordered proteins. However, the absence of a stable 3D structure and the highly dynamic nature of IDPs causes averaging of NMR chemical shifts, resulting in extensive cross-peak overlap in the NMR spectra.<sup>[5–9]</sup> Furthermore, fast hydrogen exchange of the solvent-exposed amide and other labile protons with water protons causes extensive line broadening or even complete disappearance of the corresponding resonances in the NMR spectra. Therefore, new NMR methods need to be derived or conventional techniques developed for folded proteins need to be adapted to account for the particular spectroscopic properties of IDPs.

To reduce the spectral overlap problem, uniform isotopic enrichment of the IDP with stable isotopes (<sup>13</sup>C, <sup>15</sup>N) is mandatory. Indeed, <sup>13</sup>C and <sup>15</sup>N nuclei are characterized by an

increased chemical shift dispersion with respect to protons. Therefore, proton-detected triple-resonance experiments<sup>[10,11]</sup> provide the spectral resolution required for site-resolved investigation of IDP structure, dynamics, and interaction modes.<sup>[12–14]</sup> Recently, the advent of more sensitive NMR instrumentation has brought carbon detection in the suitable sensitivity range for biomolecular NMR applications.<sup>[15–17]</sup> <sup>13</sup>C-Detected exclusively heteronuclear NMR experiments have been developed and offer valuable ways for the characterization of IDPs.<sup>[18–21]</sup>

The impact of hydrogen protein–solvent exchange processes on the NMR spectra of IDPs has never been discussed in detail, despite its importance, as most NMR experiments used to characterize IDPs are based on amide proton detection. Hydrogen exchange rates are highly dependent on the sample pH and temperature,<sup>[22]</sup> and changes in these two parameters can thus strongly influence the quality of the spectra. Inspecting the IDP literature reveals that most NMR studies have been performed at low temperatures and (slightly) acidic pH to reduce exchange-induced line broadening in the <sup>1</sup>H–<sup>15</sup>N spectra, and in triple-resonance experiments that are based on amide <sup>1</sup>H detection.

The ensemble of conformers that an IDP adopts in solution and its ability to bind to molecular partners, may be strongly dependent on the environmental conditions. Therefore, it is important to have NMR methods to access atomic-resolution information under conditions that more closely approach physiological conditions (neutral pH, body temperature). In this context, <sup>13</sup>C detection provides a valuable method of investigation as <sup>13</sup>C nuclei are not only characterized by a good chemical shift dispersion even in absence of a stable 3D structure but they are also insensitive to hydrogen-exchange-induced line broadening.<sup>[23–27]</sup> With increasing temperature and pH, the quality of 2D <sup>1</sup>H–<sup>15</sup>N correlation spectra deteriorates owing to the more efficient hydrogen-exchange mechanism, resulting in increasing number of peaks that are extensively line broadened, while at the same time the quality of the <sup>13</sup>C-detected <sup>13</sup>CO–<sup>15</sup>N spectra is maintained, if not improved. This is illustrated in Figure 1, which shows <sup>1</sup>H–<sup>15</sup>N and <sup>13</sup>CO–<sup>15</sup>N spectra recorded in the temperature range of 285.7 K to 304.8 K (pH 7.4) for the IDP  $\alpha$ -synuclein, a 140 residue human protein implicated in neurodegenerative diseases.<sup>[28]</sup> This comparison, which is a general behavior observed for IDPs, demonstrates that <sup>13</sup>C-start <sup>13</sup>C-detected experiments enable us to recover atomic resolution information that is not available from amide <sup>1</sup>H-detected experiments, thus opening new possibilities for the characterization of IDPs under close to physiological sample conditions.

[\*] T. Hošek, Prof. R. Pierattelli, Prof. I. C. Felli  
CERM and Department of Chemistry “Ugo Schiff”  
University of Florence  
Via Luigi Sacconi 6, 50019 Sesto Fiorentino, Florence (Italy)  
E-mail: felli@cerm.unifi.it

Dr. S. Gil, Dr. R. Kümmerle  
Bruker BioSpin AG  
Industriestrasse 26, 8117 Fällanden (Switzerland)  
Z. Solyom, Dr. B. Brutscher  
Institut de Biologie Structurale, Université Grenoble 1, CNRS, CEA  
Rue Jules Horowitz 41, 38027 Grenoble Cedex 1 (France)

[\*\*] We thank Drs. Melanie Schwarten and Dieter Willbold (FZ Jülich (Germany)) for their contributions to the NSSA phosphorylation study, Leonardo Gonnelli (CERM) for the  $\alpha$ -synuclein samples, and Dr. Klaus-Peter Neidig and Dr. Wolfgang Bermel (Bruker BioSpin GmbH) for stimulating discussions. This work has been supported in part by the EC Project BioNMR (Contract no 261863). S.G., T.H., and Z.S. are fellows of the IDPbyNMR Marie Curie action of the EC (Contract no 264257).



Supporting information for this article is available on the WWW under <http://dx.doi.org/10.1002/anie.201304272>.

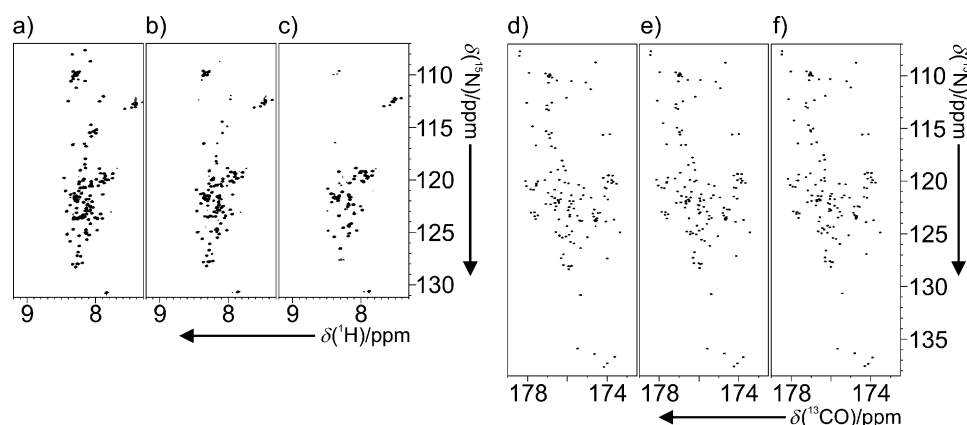


**Figure 1.** 2D spectra correlating the backbone amide nitrogen either with the directly bound amide proton or with the directly bound carbonyl. a)–c)  $^1\text{H}$ – $^{15}\text{N}$  HSQC and d)–f)  $^{13}\text{C}$ – $^{15}\text{N}$  CON acquired on  $\alpha$ -synuclein at pH 7.4 are shown as a function of increasing temperature: a), d) 285.7 K; b), e) 295.5 K; c), f) 304.8 K. Each spectrum was acquired with one scan per increment, and the same spectral resolution (in Hz) was chosen for the two experiments. Similar behaviour is observed employing different variants of 2D  $^1\text{H}$ – $^{15}\text{N}$  correlation experiments (Supporting Information, Figure S1).

A major drawback of  $^{13}\text{C}$ -detected experiments remains their low intrinsic sensitivity owing the approximately four times lower gyromagnetic ratio of  $^{13}\text{C}$  with respect to  $^1\text{H}$  ( $\gamma_{\text{C}} \approx \gamma_{\text{H}}/4$ ). Therefore, it has been proposed to use the larger  $^1\text{H}$  (instead of  $^{13}\text{C}$ ) polarization as a starting point of the coherence transfer pathways to increase the sensitivity of  $^{13}\text{C}$ -detected experiments.<sup>[15,18]</sup> The sensitivity of these  $^1\text{H}$ -start,  $^{13}\text{C}$ -detected experiments can be further improved by longitudinal  $^1\text{H}$  relaxation enhancement techniques.<sup>[29–34]</sup> These methods are based on the selective manipulation of a subset of proton spins that then relax back to thermodynamic equilibrium much faster owing to an energy transfer mechanism from the excited protons to the protons that remained unperturbed by the pulse sequence. The extent of longitudinal relaxation enhancement obtained by selective manipulation of amide  $^1\text{H}$  spins in  $\alpha$ -synuclein is shown in Figure 2.  $^1\text{H}$  polarization inversion recovery has been measured for individual amide sites by inverting different pools of  $^1\text{H}$  spins, followed by a relaxation delay, and a 2D  $^1\text{H}$ -flipCON readout sequence (Supporting Information, Figure S2) at pH 7.4 and 295.5 K (additional profiles at pH 6.4 are shown in the Supporting Information, Figure S3). Selective inversion of amide protons results in very fast  $^1\text{H}$  recovery with effective  $T_1$  time constants of about 60 ms (1.4 times the zero-crossing time point), instead of  $T_1 \approx 2$  s measured for non-selective  $^1\text{H}$  inversion. This circa 30-fold decrease in  $^1\text{H}$   $T_1$  is impressive, and much higher than what is typically observed for folded proteins with reported selective amide  $^1\text{H}$   $T_1$  of 200–400 ms compared to non-selective  $^1\text{H}$   $T_1$  of 1.0 to 1.5 s.<sup>[35,36]</sup> Our inversion recovery data also demonstrate that the major source of  $^1\text{H}$  relaxation enhancement under these experimental conditions can be attributed to hydrogen-exchange processes rather than  $^1\text{H}$ – $^1\text{H}$  dipolar interactions. The latter are responsible for the observed relaxation-enhancement effects in globular proteins,<sup>[30–32,34]</sup> as well as in IDPs studied at low temperature and acidic pH values.<sup>[14]</sup>

Inversion recovery curves also show that perturbation of the water resonance dramatically slows down recovery of amide protons to equilibrium. This has a strong impact on the performance of NMR spectra of IDPs, in particular when approaching physiological conditions. Therefore avoiding perturbation of water protons becomes a key general aspect to consider in the design of NMR spectra optimized for the study of IDPs.

The extremely short recovery times observed for amide  $^1\text{H}$  in  $\alpha$ -synuclein at close to physiological conditions prompted us to design new  $^1\text{H}$ -start  $^{13}\text{C}$ -detected experiments with minimal perturba-

tion of the water  $^1\text{H}$  spins that are expected to yield significantly improved sensitivity. A particularly useful example is the 2D  $^1\text{H}$ -BESTCON experiment shown in Figure 3a that yields “fingerprint” spectra of the protein backbone that can be used for chemical shift mapping purposes. The acronym BEST<sup>[31]</sup> refers to the use of band-selective amide  $^1\text{H}$  pulses to achieve longitudinal relaxation enhancement. The BEST technique was preferred over alternative solutions, for example, flip-back approaches, as it performs best with respect to the remaining amount of water  $^1\text{H}$  polarization after one scan. Because of the long  $^1\text{H}$   $T_1$  of water (ca. 3 s at

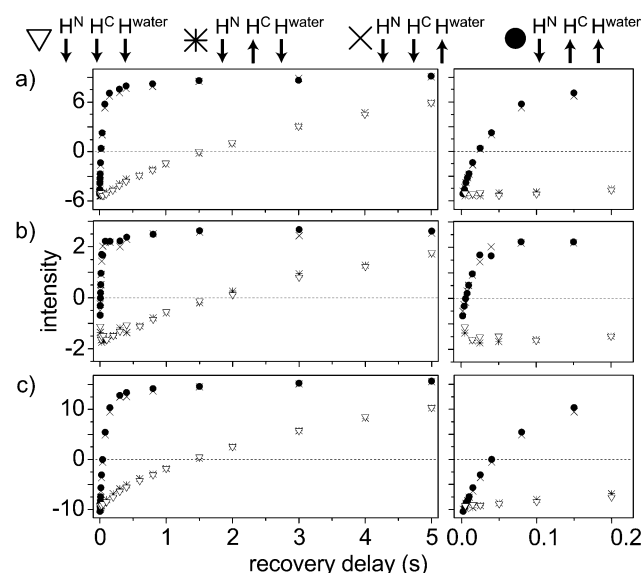


**Figure 2.** Inversion recovery profiles of amide protons acquired with the variant of the  $^1\text{H}$ -flipCON (described in the Supporting Information, Figure S2) for selected amino acids of  $\alpha$ -synuclein: a) Val 40; b) His 50; c) Leu 100. Different initial conditions are indicated as follows:  $\nabla$  non-selective,  $*$   $^1\text{H}^{\text{N}}$ – $^1\text{H}^{\text{water}}$ -selective,  $\times$   $^1\text{H}^{\text{N}}$ – $^1\text{H}^{\text{C}}$ -selective,  $\bullet$   $^1\text{H}^{\text{N}}$ -selective.

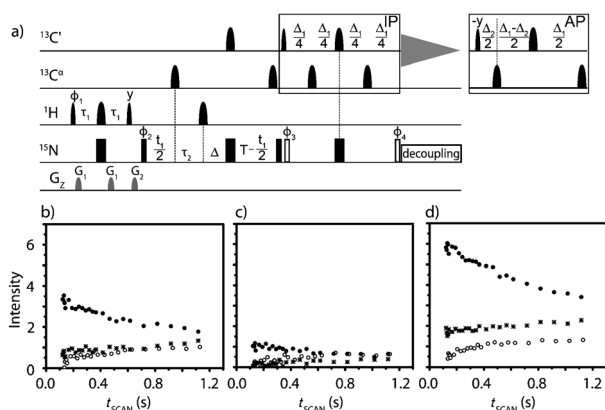


**Figure 3.** a)  $H^N\text{-BEST}^{\text{CON}}$  pulse sequence. The delays are:  $\tau_1 = 1/(4J_{\text{NH}}) - 0.5\delta_1 - 0.5\delta_2$ ,  $\tau_2 = 1/(4J_{\text{NH}}) - 0.5\delta_2$ ,  $\Delta_1 = 1/(2J_{\text{CON}})$ ,  $33.2\text{ ms}$ ,  $\Delta_2 = 1/(2J_{\text{CON}})$ ,  $9\text{ ms}$ ,  $\Delta = 1/(4J_{\text{CON}}) - 1/(4J_{\text{NH}}) - t_1/2$ ,  $T = 1/(4J_{\text{CON}})$ . The delays  $\delta_1$  and  $\delta_2$  correspond to the lengths of the PC9 and REBURP pulses that are used for  $90^\circ$  and  $180^\circ$  pulses, respectively. The phase cycle is  $\phi_1 = x, -x$ ;  $\phi_2 = 2(x), 2(-x)$ ;  $\phi_3 = 4(x), 4(-x)$ ;  $\phi_4 = 4(y), 4(-y)$ ;  $\phi_{\text{rec}} = x, -x, x, -x$ . Quadrature detection was obtained by incrementing phase  $\phi_2$  ( $t_1$ ) in States-TPPI manner. For the  $^{15}\text{N}$  virtual decoupling version, two  $90^\circ$   $^{15}\text{N}$  radio-frequency pulses are applied (white rectangles) instead of the one  $90^\circ$   $^{15}\text{N}$  rf pulse preceding IPAP block and  $^{15}\text{N}$  decoupling during acquisition. b)–d) Intensity normalized accordingly to  $T_{\text{scan}}$  time, for CON ( $\circ$ ),  $H^N\text{-start}^{\text{CON}}$  ( $\star$ ), and  $H^N\text{-BEST}^{\text{CON}}$  ( $\bullet$ ) for selected amino acids of  $\alpha$ -synuclein, b) Val 40, c) His 50, and d) Leu 100 at pH 7.4 and 295.5 K.

room temperature),<sup>[37,38]</sup> even minimal perturbation of the water  $^1\text{H}$  results in significantly reduced steady-state water  $^1\text{H}$  polarization under fast-pulsing conditions, and thus in a reduction of the longitudinal enhancement effect required for optimal sensitivity.

In fact,  $^1\text{H}$  recovery starts right after the last  $^1\text{H}$  pulse, well before the end of the pulse sequence, in contrast to  $^1\text{H}$ -detected experiments that typically end with  $^1\text{H}$  pulses. Therefore, at the end of the  $H^N\text{-BEST}^{\text{CON}}$  pulse sequence (including signal acquisition), sufficient  $^1\text{H}$  polarization may already have built up to immediately start the next scan without any additional delay. To allow for long  $^{13}\text{C}$  acquisition times to take benefit of the favorable transverse relaxation properties of IDPs, and avoid problems related to probe heating owing to  $^{15}\text{N}$  decoupling during acquisition, we have implemented virtual  $^{15}\text{N}$  decoupling in the pulse sequence.<sup>[18,39]</sup>

The performance of the new experiment in terms of sensitivity was evaluated by recording a series of 2D  $^{13}\text{C}$ – $^{15}\text{N}$  correlation spectra of  $\alpha$ -synuclein with different inter-scan delays, ranging from 0 to 1 s, using either  $H^N\text{-BEST}^{\text{CON}}$ , the analogous experiment employing non-selective  $^1\text{H}$  pulses,  $H^N\text{-start}^{\text{CON}}$ , or the  $^{13}\text{C}$ -start CON pulse schemes. The results obtained for selected residues of  $\alpha$ -synuclein are shown in Figure 3b–d. The first observation from these data is that starting with  $^1\text{H}$  as a polarization source in the  $H^N\text{-start}^{\text{CON}}$  experiment does not result in a significant sensitivity increase with respect to the  $^{13}\text{C}$ -start CON version under these experimental conditions. This is mainly explained by the long non-selective  $^1\text{H}$   $T_1$  of about 2 s compared to the  $^{13}\text{C}$   $T_1$  of about 1 s (estimated value), and by additional  $^1\text{H}$  relaxation occurring during the  $^1\text{H}$ -pulse sequence. It is interesting

to note how under these conditions, amide  $^1\text{H}$  polarization recovery for IDPs may become slower than  $^{13}\text{C}$  recovery of carbonyl nuclei. Much larger signal gains are obtained for the  $H^N\text{-BEST}^{\text{CON}}$  experiment that benefits from the extremely short selective recovery times of amide  $^1\text{H}$  that are used as starting polarization. The observed sensitivity gains ( $H^N\text{-BEST}^{\text{CON}}$  over  $^{13}\text{C}$ -start CON), determined for short recycle times of 150 ms, vary between different sites from a factor of 4 to a factor of 12 (Supporting Information, Figure S4). The example curves shown in Figure 3b–d have been chosen to be representative of residues characterized by solvent exchange rates of different magnitude. For residues characterized by (relatively) slow exchange under these conditions (for example, Leu 100), a higher sensitivity increase is observed than for residues with faster exchanging amide protons (for example, His 50). This demonstrates that starting from amide  $^1\text{H}$  introduces again a dependency on the solvent exchange rates, and that there is an optimal exchange regime for the use of such BEST-type  $^1\text{H}$ -start  $^{13}\text{C}$ -detected experiments. Maximal sensitivity is achieved if the exchange rate is large with respect to the longitudinal relaxation rate  $R_1$ , but still small compared to the transverse relaxation rate  $R_2$  ( $1\text{ s}^{-1} < k_{\text{ex}} < 10^2\text{ s}^{-1}$ ). In the presence of even faster hydrogen exchange, experimental variants exploiting  $^{13}\text{C}$ ,<sup>[23,25]</sup> or non-exchangeable  $^1\text{H}$ ,<sup>[18]</sup> as the starting polarization source are expected to yield higher sensitivity.

The  $H^N\text{-BEST}^{\text{CON}}$  experiment is particularly useful to study the behavior of IDPs inside living cells (in-cell NMR) or to monitor post-translational modifications occurring either in vitro or in vivo, because to be biologically relevant, all of these studies are preferably performed under sample conditions that are close to physiological pH and temperature.

In-cell NMR spectroscopy provides a unique spectroscopic method to investigate the fate of a protein in a cellular context. In particular, it allows changes induced by different cellular stimuli to be monitored or protein spectra obtained for different cell types to be compared.<sup>[40–44]</sup> A number of techniques, for example bacterial over-expression, injection, electroporation, or direct expression of proteins in human cells, have been developed during recent years that allow to introduce isotopic labeled protein into various cell types.<sup>[40–44]</sup> The extensive line broadening that is typical for in-cell spectra, in combination with the drastically reduced chemical shift dispersion and high solvent exchange rates of IDPs, has a strong negative impact on the amount of residue-specific information that can be obtained through 2D  $^1\text{H}$ – $^{15}\text{N}$  correlation experiments.  $^{13}\text{C}$ -detected experiments offer a valuable solution to this problem thanks to the higher chemical shift dispersion and reduced sensitivity to exchange broadening.<sup>[25,45]</sup> However, high sensitivity is required to ensure short experimental times to cope with the limited lifetime of meaningful in-cell NMR samples. The use of  $^1\text{H}$  as a starting polarization source as well as longitudinal relaxation enhancement are important features for the study of IDPs in cells through  $^{13}\text{C}$ -detected exclusively heteronuclear NMR experiments.<sup>[46]</sup> An example of an in-cell  $H^N\text{-BEST}^{\text{CON}}$  spectrum of  $\alpha$ -synuclein over-expressed in *E. coli* cells is shown in Figure 4. The inset clearly shows how the  $H^N\text{-BEST}^{\text{CON}}$  experiment enables to detect correlations that were lost

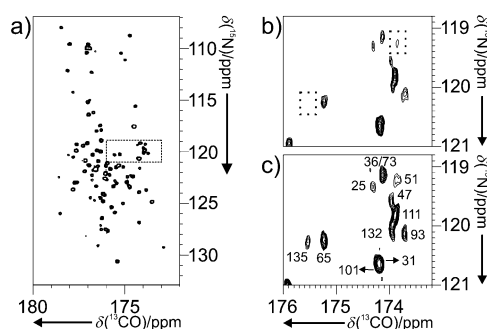


**Figure 4.** a) 2D  $^{13}\text{C}$ – $^{15}\text{N}$   $\text{H}^{\text{N-BEST}}$  CON spectrum of  $\alpha$ -synuclein in *E. coli* cells acquired in 20 min. The region of the spectrum enclosed by a rectangular box is enlarged to highlight how c)  $\text{H}^{\text{N-BEST}}$  CON enables a better sensitivity to be obtained compared to b)  $\text{H}^{\text{N-flip}}$  CON and to detect correlations that otherwise would not have been detected in the same experimental time.

under the spectral noise in the corresponding  $\text{H}^{\text{N-flip}}$  implementation of the experiment.

Another interesting application of NMR spectroscopy at nearly physiological conditions consists in following post-translational modifications modulating protein function. Among them, recent studies have focused on monitoring phosphorylation events involving intrinsically disordered proteins.<sup>[47–49]</sup> Also in this case,  $^{13}\text{C}$ -detected NMR experiments complement well the  $^1\text{H}$ -detected experiments for obtaining site-resolved information on phosphorylation events in intrinsically disordered proteins (for an example, see the Supporting Information, Figure S5).

In conclusion, we have shown here that  $^{13}\text{C}$ -start  $^{13}\text{C}$ -detected experiments do not suffer from fast hydrogen exchange between amide and solvent protons in IDP samples studied at close to physiological conditions, thus enabling us to recover information that would be difficult or even impossible to obtain through amide  $^1\text{H}$ -detected experiments. Furthermore, in favourable cases the fast hydrogen exchange rates can even be turned into a spectroscopic advantage. By combining longitudinal  $^1\text{H}$  relaxation optimized BEST-type techniques with  $^{13}\text{C}$ -direct detection pulse schemes, important sensitivity improvements can be achieved, and experimental times can be significantly reduced. This opens up new applications for monitoring chemical shift changes in IDPs upon interaction to a binding partner, chemical modification, or by changing the environment, under sample conditions that were inaccessible by conventional techniques. This concept can be easily extended to other  $^1\text{H}$ -start  $^{13}\text{C}$ -detected experiments. Furthermore,  $^{13}\text{C}$ -detected NMR experiments can be used to obtain semi-quantitative information about hydrogen-exchange rates without directly detecting the exchangeable amide  $^1\text{H}$  by quantifying the signal enhancement observed in  $\text{H}^{\text{N-BEST}}$  CON with respect to  $\text{H}^{\text{N-start}}$  CON spectra.<sup>[18,33]</sup> This may become useful to monitor changes in the exchange rates after for example, some binding event, reflecting a change in the solvent accessibility at the binding site of the IDP.

Received: May 17, 2013

Revised: July 30, 2013

Published online: September 20, 2013

**Keywords:** intrinsically disordered proteins · longitudinal relaxation enhancement · NMR spectroscopy ·  $\alpha$ -synuclein

- [1] P. E. Wright, H. J. Dyson, *J. Mol. Biol.* **1999**, 293, 321–331.
- [2] P. Tompa, M. Fuxreiter, *Trends Biochem. Sci.* **2008**, 33, 2–8.
- [3] P. Tompa, *Structure and function of intrinsically disordered proteins*, Taylor and Francis Group, Boca Raton, FL, **2009**.
- [4] V. N. Uversky, A. K. Dunker, *Biochim. Biophys. Acta Proteins Proteomics* **2010**, 1804, 1231–1264.
- [5] D. Neri, G. Wider, K. Wüthrich, *Proc. Natl. Acad. Sci. USA* **1989**, 89, 4397–4401.
- [6] H. J. Dyson, P. E. Wright, *Methods Enzymol.* **2001**, 339, 258–271.
- [7] H. Zhang, S. Neal, D. S. Wishart, *J. Biomol. NMR* **2003**, 25, 173–195.
- [8] D. Eliezer, *Curr. Opin. Struct. Biol.* **2009**, 19, 23–30.
- [9] J. Marsh, S. A. Teichmann, J. D. Forman-Kay, *Curr. Opin. Struct. Biol.* **2012**, 22, 643–650.
- [10] M. Sattler, J. Schleucher, C. Griesinger, *Prog. Nucl. Magn. Reson. Spectrosc.* **1999**, 34, 93–158.
- [11] A. Bax, S. Grzesiek, *Acc. Chem. Res.* **1993**, 26, 131–138.
- [12] M. D. Mukrasch, S. Bibow, J. Korukottu, S. Jeganathan, J. Biernat, C. Griesinger, E. Mendelkow, M. Zweckstetter, *PLoS Biol.* **2009**, 7, e34.
- [13] V. Motáčkova, J. Nováček, A. Zawadzka-Kazimierczuk, K. Kazimierczuk, L. Židek, H. Šanderová, L. Krásný, W. Koźmiński, V. Sklenář, *J. Biomol. NMR* **2010**, 48, 169–177.
- [14] Z. Solyom, M. Schwarten, L. Geist, R. Konrat, D. Willbold, B. Brutscher, *J. Biomol. NMR* **2013**, 55, 311–321.
- [15] Z. Serber, C. Richter, D. Moskau, J.-M. Boehlen, T. Gerfin, D. Marek, M. Haeblerli, L. Baselgia, F. Laukien, A. S. Stern, J. C. Hoch, V. Dötsch, *J. Am. Chem. Soc.* **2000**, 122, 3554–3555.
- [16] I. Bertini, L. Duma, I. C. Felli, M. Fey, C. Luchinat, R. Pierattelli, P. R. Vasos, *Angew. Chem.* **2004**, 116, 2307–2309; *Angew. Chem. Int. Ed.* **2004**, 43, 2257–2259.
- [17] H. Kovacs, D. Moskau, M. Spraul, *Prog. Nucl. Magn. Reson. Spectrosc.* **2005**, 46, 131–155.
- [18] W. Bermel, I. Bertini, V. Csizmek, I. C. Felli, R. Pierattelli, P. Tompa, *J. Magn. Reson.* **2009**, 198, 275–281.
- [19] W. Bermel, I. Bertini, I. C. Felli, R. Peruzzini, R. Pierattelli, *ChemPhysChem* **2010**, 11, 689–695.
- [20] J. Nováček, A. Zawadzka-Kazimierczuk, V. Papoušková, L. Židek, H. Šanderová, L. Krásný, W. Koźmiński, V. Sklenář, *J. Biomol. NMR* **2011**, 50, 1–11.
- [21] W. Bermel, I. Bertini, L. Gonnelli, I. C. Felli, W. Kozminski, A. Piai, R. Pierattelli, J. Stanek, *J. Biomol. NMR* **2012**, 53, 293–301.
- [22] Y. W. Bai, J. S. Milne, L. Mayne, S. W. Englander, *Proteins Struct. Funct. Genet.* **1993**, 17, 75–86.
- [23] W. Bermel, I. Bertini, I. C. Felli, R. Kümmerle, R. Pierattelli, *J. Magn. Reson.* **2006**, 178, 56–64.
- [24] I. Bertini, I. C. Felli, L. Gonnelli, R. Pierattelli, Z. Spyraniti, G. A. Spyroulias, *J. Biomol. NMR* **2006**, 36, 111–122.
- [25] W. Bermel, I. Bertini, I. C. Felli, Y.-M. Lee, C. Luchinat, R. Pierattelli, *J. Am. Chem. Soc.* **2006**, 128, 3918–3919.
- [26] S. T. Hsu, C. W. Bertocini, C. M. Dobson, *J. Am. Chem. Soc.* **2009**, 131, 7222–7223.
- [27] L. Skora, S. Becker, M. Zweckstetter, *J. Am. Chem. Soc.* **2010**, 132, 9223–9225.
- [28] P. H. Weinreb, W. G. Zhen, A. W. Poon, K. A. Conway, P. T. Lansbury, Jr., *Biochemistry* **1996**, 35, 13709–13715.
- [29] K. Pervushin, B. Vogeli, A. Eletsky, *J. Am. Chem. Soc.* **2002**, 124, 12898–12902.
- [30] P. Schanda, B. Brutscher, *J. Am. Chem. Soc.* **2005**, 127, 8014–8015.

- [31] P. Schanda, H. Van Melckebeke, B. Brutscher, *J. Am. Chem. Soc.* **2006**, *128*, 9042–9043.
- [32] E. Lescop, P. Schanda, B. Brutscher, *J. Magn. Reson.* **2007**, *187*, 163–169.
- [33] W. Bermel, I. Bertini, I. C. Felli, R. Pierattelli, *J. Am. Chem. Soc.* **2009**, *131*, 15339–15345.
- [34] A. Favier, B. Brutscher, *J. Biomol. NMR* **2011**, *49*, 9–15.
- [35] B. Brutscher, P. Schanda in *Encyclopedia of NMR* (Eds.: M. Grant, R. K. Harris), J. Wiley and Sons, Chichester, **2009**.
- [36] P. Schanda, *Prog. Nucl. Magn. Reson. Spectrosc.* **2009**, *55*, 238–265.
- [37] H. Y. Carr, E. M. Purcell, *Phys. Rev.* **1954**, *94*, 630–638.
- [38] H. J. Simpson, H. Y. Carr, *Phys. Rev.* **1958**, *111*, 1201–1202.
- [39] T. Kern, P. Schanda, B. Brutscher, *J. Magn. Reson.* **2008**, *190*, 333–338.
- [40] S. Reckel, F. Lohr, V. Dotsch, *ChemBioChem* **2005**, *6*, 1601–1606.
- [41] K. Inomata, A. Ohno, H. Tochio, S. Isogai, T. Tenno, I. Nakase, T. Takeuchi, S. Futaki, Y. Ito, H. Hirokai, M. Shirakawa, *Nature* **2009**, *458*, 106–109.
- [42] S. Liokatis, A. Stuetzer, S. J. Elsaesser, F. X. Theillet, R. Klingberg, B. van Rossum, D. Schwarzer, C. D. Allis, W. Fischle, P. Selenko, *Nat. Struct. Mol. Biol.* **2012**, *19*, 819–823.
- [43] F. X. Theillet, C. Smet-Nocca, S. Liokatis, R. Thongwichian, J. Kosten, M. K. Yoon, R. W. Kriwacki, I. Landrieu, G. Lippens, P. Selenko, *J. Biomol. NMR* **2012**, *54*, 217–236.
- [44] L. Banci, L. Barbieri, I. Bertini, E. Luchinat, E. Secci, Y. Zhao, A. R. Aricescu, *Nat. Chem. Biol.* **2013**, *9*, 297–299.
- [45] A. Binolfi, F. X. Theillet, P. Selenko, *Biochem. Soc. Trans.* **2012**, *40*, 950–954.
- [46] I. Bertini, I. C. Felli, L. Gonnelli, V. M. V. Kumar, R. Pierattelli, *Angew. Chem.* **2011**, *123*, 2387–2389; *Angew. Chem. Int. Ed.* **2011**, *50*, 2339–2341.
- [47] G. Lippens, L. Amniai, M. R. Wieckowski, A. Sillen, A. Leroy, I. Landrieu, *Biochem. Soc. Trans.* **2012**, *40*, 698–703.
- [48] F. X. Theillet, H. M. Rose, S. Liokatis, A. Binolfi, R. Thongwichian, M. Stuiiver, P. Selenko, *Nat. Protoc.* **2013**, *8*, 1416–1432.
- [49] I. Amata, M. Maffei, A. Igea, M. Gay, M. Vilaseca, A. R. Nebreda, M. Pons, *ChemBioChem* **2013**, DOI: 10.1002/cbic.201300139.